Astronomy & Astrophysics manuscript no. wasp21˙v6˙wc8
April 13, 2010

WASP-21b: a hot-Saturn exoplanet transiting a thick disc star⋆

Bouchy, F.[1,2], Hebb, L.[3,5], Skillen, I.[4], Collier Cameron, A.[5], Smalley, B.[6], Udry, S.[7], Anderson, D.R.[6], Boisse, I.[1], Enoch, B.[5], Haswell, C.A.[8], Hébrard, G.[1], Hellier, C.[6], Joshi, Y.[9], Kane, S.R.[10], Maxted, P.F.L.[6], Mayor, M.[7], Moutou, C.[11], Pollacco, D.[9], Queloz, D.[7], Simpson, E.K.[9], Smith, A.M.S.[6], Stempels, H.C.[12], Street, R.[13], Triaud, A.H.M.J.[7], and West, R.G.[14]

[1] Institut d'Astrophysique de Paris, UMR7095 CNRS, Université Pierre & Marie Curie, 98bis Bd Arago, 75014 Paris, France
[2] Observatoire de Haute-Provence, CNRS/OAMP, 04870 St Michel l'Observatoire, France
[3] Department of Physics and Astronomy, Vanderbilt University, Nashville, TN 37235, USA
[4] Isaac Newton Group of Telescopes, Apartado de Correos 321, E-38700 Santa Cruz de la Palma, Tenerife, Spain
[5] SUPA, School of Physics and Astronomy, University of St Andrews, North Haugh, St Andrews, Fife KY16 9SS, UK
[6] Astrophysics Group, Keele University, Staffordshire, ST5 5BG, UK
[7] Observatoire de Genève, Université de Genève, 51 Ch. des Maillettes, 1290 Sauverny, Switzerland
[8] Department of Physics and Astronomy, The Open University, Milton Keynes, MK7 6AA, UK
[9] Astrophysics Research Centre, School of Mathematics and Physics, Queen's University, University Road, Belfast, BT7 1NN, UK
[10] NASA Exoplanet Science Institute, Caltech, MS 100-22, 770 South Wilson Avenue, Pasadena, CA 91125, USA
[11] Laboratoire d'Astrophysique de Marseille, 38 rue Frédéric Joliot-Curie, 13388 Marseille cedex 13, France
[12] Department of Physics and Astronomy, Uppsala University, Box 516, 75120 Uppsala, Sweden
[13] Las Cumbres Observatory, 6740 Cortona Drive Suite 102, Goleta, CA 93117, USA
[14] Department of Physics and Astronomy, University of Leicester, Leicester, LE1 7RH

Received ; accepted

ABSTRACT

We report the discovery of WASP-21b, a new transiting exoplanet discovered by the Wide Angle Search for Planets (WASP) Consortium and established and characterized using the FIES, SOPHIE, CORALIE and HARPS fiber-fed echelle spectrographs. A 4.3-d period, 1.1% transit depth and 3.4-h duration are derived for WASP-21b using SuperWASP-North and high precision photometric observations at the Liverpool Telescope. Simultaneous fitting to the photometric and radial velocity data using a Markov Chain Monte Carlo procedure leads to a planet in the mass regime of Saturn. With a radius of 1.07 R_{Jup} and mass of 0.30 M_{Jup}, WASP-21b has a density close to 0.24 ρ_{Jup} corresponding to the distribution peak at low density of transiting gaseous giant planets. With a host star metallicity $[Fe/H]$ of -0.46, WASP-21b strengthens the correlation between planetary density and host star metallicity for the four known Saturn-like transiting planets. Furthermore there are clear indications that WASP-21b is the first transiting planet belonging to the thick disc.

Key words. planetary systems – techniques: photometric – Techniques : radial velocities

1. Introduction

Observations of planets that transit their host star represent the current best opportunity to test models of exoplanet structure and evolution. These last ten years, the photometric surveys have leading to an increasing list of transiting planets. About seventy transiting planetary systems have been identified from Super-Earth to Jupiter-like planets. The WASP project operates two identical instruments, at La Palma in the Northern hemisphere, and at Sutherland in South Africa in the Southern hemisphere and led these last years to the detection of about 30% of known transiting planets. Each WASP telescope has a field of view of just under 500 square degrees. The WASP survey is sensitive to planetary transit signatures in the light-curves of stars in the magnitude range V ∼ 9-13. A detailed description of the telescope hardware, observing strategy and pipeline data analysis is given in Pollacco et al. (2006).

In this paper we present the WASP photometry of SWASPJ230958.23+182346.0, high precision photometric follow-up observations with the RISE instrument on the Liverpool Telescope and high-precision radial velocity (RV) observations with the SOPHIE (1.93-m OHP), CORALIE (1.2-m La Silla) and HARPS (3.6-m La Silla) fiber-fed echelle spectrographs. These observations lead to the discovery of WASP-21b, a hot-Saturn transiting exoplanet.

2. Observations

2.1. SuperWASP observation

SuperWASP-North is a multi-camera telescope system located in La Palma and consisting of 8 Canon 200-mm f/1.8 lenses each coupled to e2v 2048×2048 pixel back illuminated CCDs (Pollacco et al. 2006). This combination of lens and camera yields a field of view of $7^o.8 \times 7^o.8$ with an angular size of 13.7 arcsec per pixel. The target SWASPJ230958.23+182346.0 was monitored from July 22th to November 27th 2006 totaling

⋆ Based on observations made with the SuperWASP-North camera hosted by the Isaac Newton Group on La Palma, the FIES spectrograph on the Nordic Optical Telescope, the CORALIE spectrograph on the 1.2-m Swiss telescope on La Silla Observatory, the SOPHIE spectrograph on the 1.93-m telescope on Haute Provence Observatory and the HARPS spectrograph on the 3.6-m ESO telescope at La Silla Observatory under programs 081.C-0388, 082.C-0040, 084.C-0185.

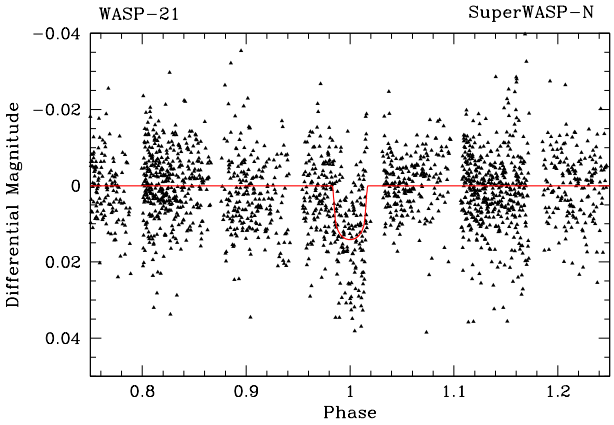

Fig. 1. Un-binned SuperWasp folded light curve for WASP-21 using the ephemeris P=4.32 days and T0=2454743.04185.

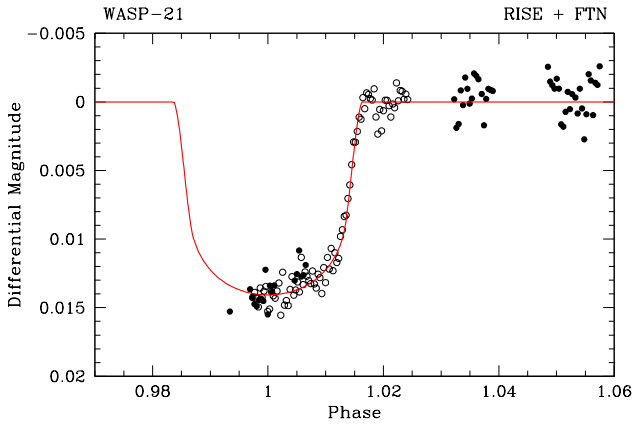

Fig. 2. Phase-folded light curve from the RISE (open circle) and FTN (black circle) photometry for WASP-21 superposed with the MCMC solutions. The RISE photometry was binned 2-minutes in time.

3814 photometric measurements. The pipeline-processed data were detrended and searched for transits using the methods described in Collier Cameron et al. (2006), yielding a detection of a periodic transit-like signature with a period of 4.32 days. Figure 1 shows the un-binned SuperWASP phase-folded light curve of WASP-21 using the ephemeris P=4.32 days and T0=2454743.04185.

2.2. Higher precision photometric Follow-up

On-off photometric observations were made with the 2-m Faulkes Telescope North (FTN) at Hawaii on 2th September 2008 using the Pan-STARRS-z broad-band filter. These observations allowed to confirm the transit signal. Follow-up photometry was performed with the fast read-out camera RISE located on the 2.0-m Liverpool Telescope at La Palma. Although the night was non-photometric and the sky was variable, a partial transit was observed on 7th October 2008 in agreement with the SuperWasp and FTN photometry. The phase-folded lightcurve of FTN and RISE are shown in Figure 2.

On October 2009, Out-of-transit high-angular resolution images were provided on the 4.2-m WHT with the Adaptive Optic NAOMI and the IR imager INGRID. Ks-band images have a FWHM of 0.18 arcsec with circular contours, excluding evidence of a visible companion on that spatial scale.

2.3. Doppler follow-up

Three spectra were first obtained at the end of December 2007 with the FIES spectrograph at the 2.6-m Nordic Optical Telescope (NOT - La Palma). The combined spectrum indicated a dwarf star and the radial velocities showed no variations greater than 100 $\mathrm{m\,s^{-1}}$ excluding a low-mass star companion. RV follow-up of WASP-21 was conducted with the echelle spectrograph SOPHIE at the 1.93-m telescope of Observatoire de Haute Provence (Perruchot et al. 2008, Bouchy et al. 2009), CORALIE at the 1.2-m Swiss Euler telescope of La Silla (Queloz et al. 2000), and HARPS at the 3.6-m telescope of ESO La Silla (Mayor et al. 2003). A total of eleven SOPHIE measurements were made on July and August 2008 with about the same signal-to-noise ratio S/N=30 in order to minimize the Charge Transfer Inefficiency (CTI) effect (Bouchy et al. 2009) although it is now corrected by the Data Reduction Software. Some measurements were made with moon light but without significant effect on the RV measurements considering that the RV of the target (-89.4 $\mathrm{km\,s^{-1}}$) was always far from the moon RV. The RV uncertainties were computed assuming photon noise plus 15 $\mathrm{m\,s^{-1}}$ quadratically added in order to take into account the systematics of the High Efficiency mode like the guiding and centering errors (Boisse et al. 2010) and wavelength calibration uncertainty. Five CORALIE measurements were made simultaneously with those of SOPHIE and eight additional ones were made one year after in June and September 2009. One CORALIE point was made close to the transit epoch (BJD=2454686.83) and may be affected by the Rossiter-McLaughlin effect. We did not use it to determine the Keplerian solution. However, considering the small $v \sin i$ (≤ 2 $\mathrm{km\,s^{-1}}$) of the star, the expected amplitude of the RM effect should be lower than 20 $\mathrm{m\,s^{-1}}$ which makes it difficult to detect with CORALIE or SOPHIE. Nine HARPS measurements were made in September and October 2008 to definitively secure the candidate considering the small RV amplitude observed by SOPHIE and CORALIE, as well as to exclude blended eclipsing binaries scenario and to provide a high S/N spectrum for stellar parameters analysis (see Section 3.1). Six HARPS measurements were added in October 2009 to check for eccentricity and for additional companion in the system.

The phase-folded RVs in Figure 3 shows the SOPHIE (black circles), HARPS (red squares), CORALIE (green triangles) and FIES (blue open circles) points. All are phase matched pretty well with the photometry. The best Keplerian fit was obtained with an RV offset from the HARPS data of +11, -20.5 and +15 $\mathrm{m\,s^{-1}}$ for the CORALIE, SOPHIE and FIES data respectively. The semi-amplitude of the RV curve is K=37.2±1.1 $\mathrm{m\,s^{-1}}$. We adjust the Keplerian orbit fixing the eccentricity to zero. There is no obvious evidence for eccentricity, although it is difficult to fit for the eccentricity with a small amount of data points coming from 4 different instruments since we already have 3 other free parameters (the zero-point offsets of the RV data sets).

No significant RV drift was detected with HARPS on the time scale of 1 year excluding additional Jupiter-like companion with period less than 1 year.

The figure 4 shows the bisector span versus RV. SOPHIE and CORALIE bisector spans have uncertainties a bit larger to check their possible correlation with radial velocities. HARPS bisector spans definitively show no correlation, excluding scenarios of blended eclipsing binaries.

Table 1. Radial velocities of WASP-21

BJD -2 400 000	RV (km s^{-1})	$\pm 1\sigma$ (km s^{-1})
FIES - 2.6m NOT		
54462.336	-89.504	0.027
54465.371	-89.409	0.036
54466.364	-89.444	0.029
SOPHIE - 1.93m OHP		
54659.5872	-89.409	0.018
54662.5947	-89.418	0.018
54663.5749	-89.392	0.017
54665.5826	-89.449	0.019
54666.5773	-89.458	0.017
54667.5790	-89.387	0.017
54668.5925	-89.381	0.020
54679.5940	-89.474	0.018
54683.6242	-89.495	0.018
54685.5591	-89.393	0.018
54688.5479	-89.445	0.018
CORALIE - 1.2m Euler		
54624.9095	-89.427	0.013
54661.7883	-89.487	0.012
54662.8643	-89.475	0.014
54684.8541	-89.442	0.012
54686.8333	-89.430	0.014
55001.9020	-89.424	0.014
55009.8829	-89.398	0.015
55013.8951	-89.431	0.015
55093.6551	-89.506	0.016
55095.6656	-89.444	0.013
55096.6795	-89.407	0.014
55098.6554	-89.500	0.013
55130.6417	-89.433	0.015
HARPS - 3.6m ESO		
54706.7464	-89.4001	0.0100
54709.7655	-89.4792	0.0033
54710.7472	-89.4287	0.0038
54749.6611	-89.4309	0.0036
54754.6434	-89.4154	0.0031
54755.6635	-89.4317	0.0025
54760.6340	-89.4639	0.0022
54761.6280	-89.4782	0.0027
54763.5963	-89.4040	0.0031
55111.6377	-89.4797	0.0029
55112.6342	-89.4361	0.0032
55113.6229	-89.4118	0.0027
55115.6429	-89.4892	0.0050
55116.6385	-89.4655	0.0023
55117.6204	-89.4184	0.0045

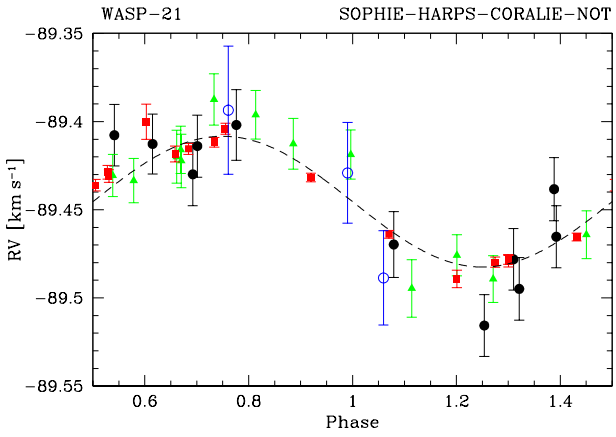

Fig. 3. Phase-folded radial velocities of WASP-21 obtained with SOPHIE (black circles), HARPS (red squares), CORALIE (green triangles) and FIES (blue open circles)

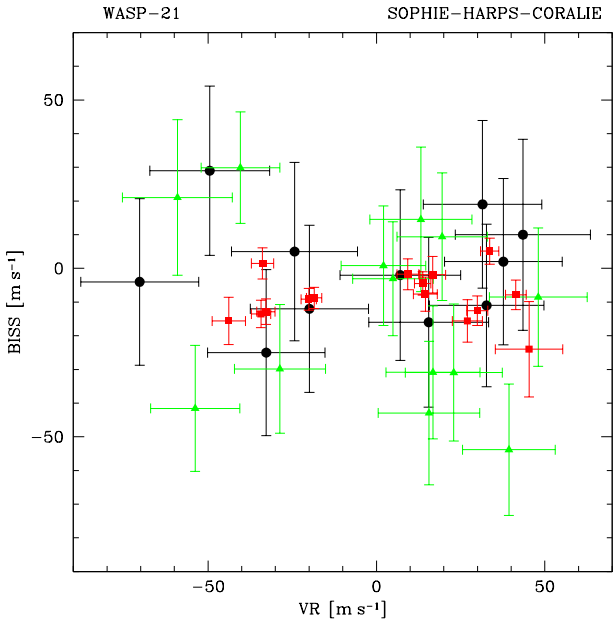

Fig. 4. Bisector span versus radial velocities of WASP-21 obtained with SOPHIE (black circles), HARPS (red squares) and CORALIE (green triangles) showing no significant correlation and excluding scenarios of blended eclipsing binaries.

3. Results and parameters

3.1. spectral classification

A detailed spectroscopic analysis of the stellar atmospheric properties was made using the FIES and HARPS spectra. We merged the HARPS spectra into one high-quality spectrum in order to perform a detailed spectroscopic analysis of the stellar atmospheric properties. This merged spectrum was continuum normalized with a low-order polynomial to retain the shape of the broadest spectral features. The total signal-to-noise ratio of the combined spectrum was about 100 per pixel.

As previously undertaken for our analysis of WASP-1 (Stempels et al. 2007) and WASP-3 (Pollacco et al. 2008), we employed the methodology of Valenti & Fischer (2005), using the same tools, techniques and model atmosphere grid. We used the package Spectroscopy Made Easy (SME) (Valenti & Piskunov 1996), which combines spectral synthesis with multidimensional χ^2 minimization to determine which atmospheric parameters best reproduce the observed spectrum of WASP-21 (effective temperature T_{eff}, surface gravity $\log g$, metallicity $[M/H]$, projected $v \sin i$, microturbulence *v_mic* and the macroturbulence *v_mac*). The parameters we obtained from this analysis are listed in Table 2.

The properties of WASP-21 suggest it is a member of the thick disc component of the Galaxy. Using the NOMAD catalog proper motions (Zacharias et al. 2004) and the measured systemic radial velocity, we calculate its U, V, and W space motion to be -32.8, -66.2, +61.7 km s^{-1} relative to the Sun, adopting a distance of 230 ± 50 pc based on the measured V band magnitude (V = 11.58 ± 0.08) and the absolute V magnitude of a

typical G3V type star (Gray 1988). It is clear that WASP-21 is lagging behind the Sun (which moves with the thin disc) with a large negative V velocity similar to the canonical thick disc value of $\sim$ -45 km s^{-1} (Morrison et al. 1990). WASP-21 is also metal poor with $[M/H] = -0.4 \pm 0.1$, again similar to the mean thick disc value of ~ -0.6 dex.

In addition, the abundance analysis shows enhanced α/Fe ratios which is also typical of a thick disc star (see Edvardsson et al. 1993). The alpha elements, Mg Ca, Ti, and Si have abundances of $\sim$-0.25, approximately twice the value of iron, $[Fe/H]$ =-0.46, and the other iron peak elements ($[V/H]$=-0.32, $[Cr/H]$=-0.44, $[Mn/H]$=-0.75, $[Co/H]$=-0.39 and $[Ni/H]$=-0.46).

Furthermore, when we compare the effective temperature (T_{eff} = 5800 ± 100 K), metallicity and mean stellar density ($\rho/\rho_{\odot}$ = 0.84) derived from the transit parameters of WASP-21 to theoretical stellar evolution models from Girardi et al. (2000) as described in Hebb et al. (2009), we find the star to be evolved off the zero-age main sequence and similar in age to that of the thick disc (age $\sim 12 \pm 5$ Gyr).

In order to quantify the probability that WASP-21 is a member of the thick disc, we compare its chemical and kinematic properties to the properties of similar model stars in the Besançon Galactic model (Robin et al. 2003) where the population class of the stars are known. We select a set of model main sequence stars in a small volume around the position of WASP-21 for comparison. We generate over 800,000 model stars in 55 realizations of the simulation which have spectral types of F5V-K7V, distances of 150-600 pc, and positions within ±5° in each direction of WASP-21 (l = 92,b = −38). The model stars come from all the Galactic components and are not selected based on their velocities or metallicities. Of the model stars with metallicities between -0.5 and -0.3 dex and within ±15 km s^{-1} of the calculated U,V, and W values of WASP-21, all have ages $\geq$ 7 Gyr (population class 7 and 8) suggesting WASP-21 is old. Furthermore, 92% of the matching model stars are belonging to the thick disc.

In summary, WASP-21 has a high probability of being a thick disc member based on its kinematic properties, low metallicity, abundance patterns, and likely old age.

3.2. Planet parameters

To determine the planetary and orbital parameters the radial velocity measurements were combined with the photometry from WASP, RISE and FTN in a simultaneous fit using the Markov Chain Monte Carlo (MCMC) technique. The details of this process are described in Pollacco et al. (2008). Recent features and improvements were included. The linear de-trending of the optical light curves is made with respect to phase at each step in the MCMC chain. An initial fit showed that the orbital eccentricity was poorly constrained by the available data and nearly consistent with zero. We therefore fixed the eccentricity parameter at zero. We derived the host star mass consistently within the MCMC code by comparing the mean stellar density (measured from the shape of the transit) and the observed metallicity and effective temperature of the host star to an empirical relation defined by a set of detached eclipsing binaries with component masses and radii measured to high precision ($\leq$ 3%) (Torres et al. 2010). Using this novel technique, we derived a mass for WASP-21 of $M = 1.01 \pm 0.025 M_{\odot}$. The mass and radius of WASP-21b, given in Table 3 with the other best-fit parameters, are then found to be M_P= 0.30±0.01 M_{Jup} and R_P = 1.07±0.05 R_{Jup}, respectively.

Table 2. Stellar parameters for WASP-21 derived from FIES and HARPS spectroscopy.

Parameter	WASP-21
RA (J2000)	23 09 58.23
DEC (J2000)	+18 23 46.0
V	11.6
Distance	230 ± 30 pc
T_{eff}	5800 ± 100 K
$\log g$	4.2 ± 0.1
$[M/H]$	-0.4 ± 0.1
$v \sin i$	1.5 ± 0.6 km/s
v_{rad}	-89.45 km s^{-1}
log A(Li)	2.19 ± 0.09
$[Na/H]$	-0.47 ± 0.11
$[Mg/H]$	-0.28 ± 0.08
$[Ca/H]$	-0.25 ± 0.13
$[Ti/H]$	-0.28 ± 0.10
$[Mn/H]$	-0.75 ± 0.14
$[Fe/H]$	-0.46 ± 0.11
$[Si/H]$	-0.25 ± 0.12
$[Sc/H]$	-0.33 ± 0.11
$[V/H]$	-0.32 ± 0.10
$[Cr/H]$	-0.44 ± 0.17
$[Co/H]$	-0.39 ± 0.14
$[Ni/H]$	-0.46 ± 0.14

Finally, we would like to note that the host star mass derived from the theoretical stellar evolution models of Girardi et al. (2000) is significantly less than what we find using the empirical relation even though we use the same observed stellar density, temperature and metallicity. Upon further investigation, we find that the metallicity has a strong effect on the radii and effective temperatures of the theoretical stars that is not present in the observed eclipsing binary systems. Specifically, a $\sim$ 5800 K, solar metallicity (Z = 0.019) theoretical star with an age of 5 Gyr has a predicted mass of $1.0 M_{\odot}$, but at Z = 0.008 ($[M/H] = -0.37$), the predicted mass is $\sim$ 10% less ($0.9 M_{\odot}$). However, the four eclipsing binary components in Torres et al. (2010) with temperatures within ±100 K of WASP-21, have [Fe/H] measurements ranging from -0.1 to +0.24, but masses similar to within 5%. There is a clear difference between the predicted effects of metallicity on the properties of stars and the observed effects in eclipsing binaries. Using a stellar mass of $0.9 M_{\odot}$ leads to a planetary mass and radius for WASP-21b of M_P= 0.29±0.01 M_{Jup} and R_P = 1.03±0.05 R_{Jup}, respectively, $\sim$ 3% less than our adopted value.

4. Discussion and conclusion

Figure 5 shows the mass-radius diagram of known gaseous giant transiting exoplanets. WASP-21b is part of the only 4 transiting gas-giant planets with mass below 0.4 M_{Jup} including HAT-P-12b (Hartman et al. 2009), HD149026b (Sato et al. 2005) and WASP-29b (Hellier et al. 2010).

Figure 6 shows the density histogram of transiting gas-giant planets with mass in between 0.2 and 1.5 Jupiter mass (totaling 45 exoplanets). The probability density function presents a clear asymmetric distribution peaking at the lowest densities (0.25 ρ_{Jup}) and decreasing from 0.25 to 1.25 ρ_{Jup}. WASP-21b and HAT-P-12b, with both a density of $\sim$ 0.24 ρ_{Jup}, are bloated planet with a density lying close to the mode of that distribution. Only four transiting exoplanets with mass in the range 0.2-1.5 M_{Jup} have density greater than or equal to Jupiter including the Saturn-like planet HD149026b as well as WASP-7b (Hellier et

Table 3. WASP-21 system parameters and 1σ error limits derived from the MCMC analysis.

Parameter	Value
Transit epoch T_0 [HJD]	$2454743.04185^{+0.0019}_{-0.0022}$
Orbital period P [days]	$4.322482^{+0.000019}_{-0.000024}$
Planet/star area ratio $(R_p/R_*)^2$	$0.0108^{+0.00037}_{-0.00035}$
Transit duration t_T [days]	$0.140^{+0.0048}_{-0.0040}$
Impact parameter b [R_*]	$0.23^{+0.12}_{-0.15}$
Orbital inclination I [degrees]	$88.75^{+0.84}_{-0.70}$
Stellar reflex velocity K [km s^{-1}]	$0.0372^{+0.0010}_{-0.0011}$
Orbital semimajor axis a [AU]	$0.052^{+0.00041}_{-0.00044}$
Stellar mass M_* [$M_\odot$]	$1.01^{+0.024}_{-0.025}$
Stellar radius R_* [$R_\odot$]	$1.06^{+0.04}_{-0.04}$
Stellar surface gravity $\log g_*$ [cgs]	$4.39^{+0.028}_{-0.028}$
Stellar density ρ_* [$\rho_\odot$]	$0.84^{+0.09}_{-0.08}$
Planet radius R_p [R_J]	$1.07^{+0.05}_{-0.05}$
Planet mass M_p [M_J]	$0.300^{+0.010}_{-0.010}$
Planet density ρ_p [ρ_J]	$0.242^{+0.035}_{-0.032}$

al. 2008) and OGLE-TR-113b (Bouchy et al. 2004). The density of the four Saturn-like transiting planets appears clearly correlated with the metallicity of their host stars ([Fe/H]=-0.46, -0.29, +0.11, and +0.36 for WASP-21b and HAT-P-12b, WASP-29b, and HD149026b respectively) confirming and reinforcing the relation established by Guillot et al. (2006).

It is clear from previous studies that thick disc stars do form planets which means that planet formation was ongoing when the Milky Way was still relatively young (i.e. as early as $\sim$ 12 Gyr ago) and that these planetary systems have survived the process (i.e. major merger with a satellite galaxy) that formed the thick disc. In particular, Reid et al. (2007 identify five previously known exoplanet host stars which are likely thick disc members based on their subsolar metallicities, relatively large space motions (compared to the Sun) and high [α/Fe] ratios. More recently, Neves et al. (2009) identified 5 planet-host stars belonging to the thick disc from the 451 stars from the HARPS GTO planet search program indicating that approximately 17% of the thick disc stars are planet hosts. They found some indication that metal-poor ([Fe/H] $\leq$ -0.2) planet-host stars originate preferentially in the thick disc, as also suggested by Haywood (2008). WASP-21b is the first transiting planet with a measured radius and definitive mass to orbit a member of this population.

Acknowledgements. The WASP Consortium comprises astronomers primarily from the Universities of Keele, Leicester, The Open University, Queen's University Belfast, the University of St Andrews, the Isaac Newton Group (La Palma), the Instituto de Astrofisica de Canarias (Tenerife) and the South African Astronomical Observatory. The SuperWASP-N camera is hosted by the Isaac Newton Group on La Palma with funding from the UK Science and Technology Facilities Council. We extend our thanks to the Director and staff of the Isaac Newton Group for their support of SuperWASP-N operations. Based in part on observations made at Observatoire de Haute Provence (CNRS), France, and on observations made with the Nordic Optical Telescope, operated on the island of La Palma jointly by Denmark, Finland, Iceland, Norway, and Sweden, in the Spanish Observatorio del Roque de los Muchachos of the Instituto de Astrofisica de Canarias. We wish to thank the "Programme National de Planétologie" (PNP) of CNRS/INSU, the Swiss National Science Foundation, and the French National Research Agency (ANR-08-JCJC-0102-01) for their continuous support to our planet-search programs. FB would like to acknowledges PLS for continuous support and advice.

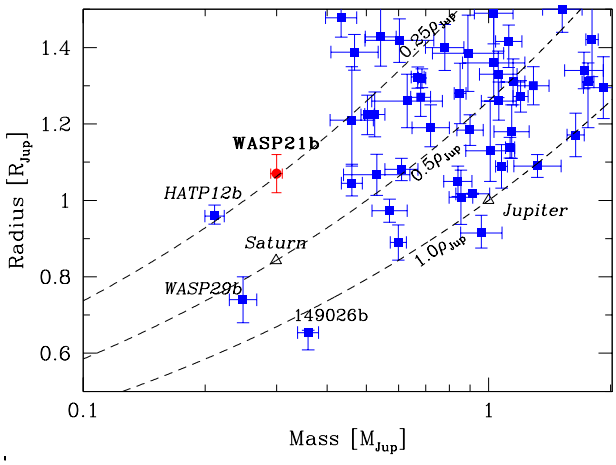

Fig. 5. Mass-radius diagram of transiting gaseous giant exoplanets ($M_P \geq 0.1$ M_{Jup}).

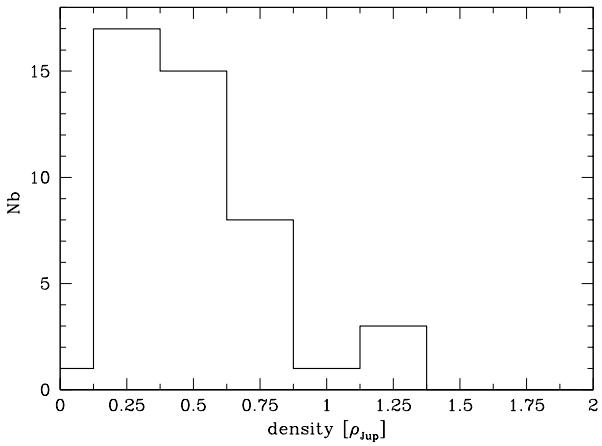

Fig. 6. Histogram of density of transiting hot-Jupiters with mass in the range 0.2-1.5 M_{Jup}.

References

Boisse, I., Bouchy, F., Chazelas, B., et al., 2010, in New technologies for probing the diversity of brown dwarfs and exoplanets, EPJ Web of Conferences, in press
Bouchy, F., Pont, F., Santos, N.C., et al., 2004, A&A, 421, L13
Bouchy, F., Hébrard, G., Udry, S., et al., 2009, A&A, 505, 853
Collier Cameron, A., Pollacco, D., Street, R.A., et al., 2006, MNRAS, 373, 799
Edvardsson, B., Andersen, J., Gustafsson, B., et al., 1993, A&A, 275, 101
Girardi, L., Bressan, A., Bertelli, G., & Chiosi, C. 2000, A&AS, 141, 371
Gray, D.F., 1988, Lectures on Spectral-line Analysis: F, G, and K Stars (Arva, Ontario: Publisher)
Guillot, T., Santos, N.C, Pont, F., et al., 2006, A&A, 453, L21
Hartman, J., Bakos, G., Torres, G., et al., 2009, ApJ, 706, 785
Haywood, M., 2008, A&A, 482, 673
Hebb, L., Collier-Cameron, A., Triaud, A.H.M.J., et al. 2009, ApJ, 693, 1920
Hellier, C., Anderson, D.R., Gillon, M., et al., 2008, ApJ, 690, L89
Hellier, C., Anderson, D.R., Collier Cameron, A., et al., 2010, ApJ, submitted
Mayor, M., Pepe, F., Queloz, D., et al., 2003, Messenger, 114, 20
Morrison, H. L., Flynn, C., & Freeman, K. C. 1990, AJ, 100, 1191
Neves, V., Santos, N.C., Sousa, S.G., et al., 2009, A&A, 497, 563
Perruchot, S., Kohler, D., Bouchy, F., et al., 2008, in *Ground-based and Airborn Instrumentation for Astronomy II*, Edited by McLean, I.S., Casali, M.M., Proceedings of the SPIE, vol. 7014, 70140J
Pollacco, D.L., Skillen, I., Cameron, A.C., et al., 2006 ,PASP, 118, 1407
Pollacco, D., Skillen, I., Collier Cameron, A., et al., 2008, MNRAS, 385, 1576
Queloz, D., Mayor, M., Webber, L., et al., 2000, A&A, 354, 99
Reid, I.N., Turner, E.L., Turnbull, M.C., et al., 2007, ApJ, 665, 767
Robin, A. C., Reylé, C., Derrière, S., & Picaud, S. 2003, A&A, 409, 523
Sato, B., Fischer, D., Henry, G., et al., 2005, ApJ, 633, 465

Stempels, H.C., Collier Cameron, A., Hebb L., et al., 2007, MNRAS, 379, 773
Torres, G., Andersen, J. & Gimenez, A., 2010, A&ARv, 18, 67
Valenti, J.A., & Piskunov, N., 1996, A&AS, 118, 595
Valenti, J.A., & Fisher, D., 2005, ApJS, 159, 141
Zacharias, N., Monet, D. G., Levine, S. E., et al., 2004, Bulletin of the American Astronomical Society, 36, 1418